Development of an inflammation imaging tracer, ^{111}In-DOTA-DAPTA, targeting chemokine receptor CCR5 and preliminary evaluation in an ApoE$^{-/-}$ atherosclerosis mouse model

Lihui Wei, PhD,[a,b,c] Julia Petryk,[b,c] Chantal Gaudet, BSc,[b] Maryam Kamkar, PhD,[b] Wei Gan, PhD,[b,c] Yin Duan, MSc,[b,c] and Terrence D. Ruddy, MD[b,c]

[a] Nordion Inc., Ottawa, ON, Canada
[b] Division of Cardiology, Department of Medicine, University of Ottawa Heart Institute, Ottawa, ON, Canada
[c] Nordion Lab, Canadian Molecular Imaging Center of Excellence (C-MICE), University of Ottawa Heart Institute, Ottawa, ON, Canada

Received May 26, 2017; accepted Jan 17, 2018
doi:10.1007/s12350-018-1203-1

Background. **Chemokine receptor 5 (CCR5) plays an important role in atherosclerosis. Our objective was to develop a SPECT tracer targeting CCR5 for imaging plaque inflammation by radiolabeling D-Ala-peptide T-amide (DAPTA), a CCR5 antagonist, with ^{111}In.**

Methods. **1,4,7,10-tetraazacyclododecane-1,4,7,10-tetraacetic acid (DOTA) conjugated DAPTA (DOTA-DAPTA) was labeled with ^{111}In. Cell uptake studies were conducted in U87-CD4-CCR5 and U87-MG cells. Biodistribution was determined in C57BL/6 mice. Autoradiography, *en face* and Oil Red O (ORO) imaging studies were performed in ApoE$^{-/-}$ mice.**

Results. **DOTA-DAPTA was radiolabeled with ^{111}In with high radiochemical purity (> 98%) and specific activity (70 MBq·nmol). ^{111}In-DOTA-DAPTA exhibited fast blood and renal clearance and high spleen uptake. The U87-CD4-CCR5 cells had significantly higher uptake in comparison to the U87-MG cells. The cell uptake was reduced by three times with DAPTA, indicating the receptor specificity of the uptake. Autoradiographic images showed significantly higher lesion uptake of ^{111}In-DOTA-DAPTA in ApoE$^{-/-}$ mice than that in C57BL/6 mice. The tracer uptake in 4 month old ApoE$^{-/-}$ high fat diet (HFD) mice with blocking agent was twofold lower than the same mice without the blocking agent, demonstrating the specificity of the tracer for the CCR5 receptor.**

Conclusion. **^{111}In-DOTA-DAPTA, specifically targeting chemokine receptor CCR5, is a potential SPECT agent for imaging inflammation in atherosclerosis. (J Nucl Cardiol 2019;26:1169–78.)**

Key Words: ^{111}In-DOTA-DAPTA • CCR5 • atherosclerosis • ApoE$^{-/-}$ mice • autoradiography

Electronic supplementary material The online version of this article (https://doi.org/10.1007/s12350-018-1203-1) contains supplementary material, which is available to authorized users.

The authors of this article have provided a PowerPoint file, available for download at SpringerLink, which summarises the contents of the paper and is free for re-use at meetings and presentations. Search for the article DOI on SpringerLink.com.

Reprint requests: Lihui Wei, PhD, Nordion Lab, Canadian Molecular Imaging Center of Excellence (C-MICE), University of Ottawa Heart Institute, 40 Ruskin Street, Ottawa ON, K1Y 4W7, Canada; *lihuiwei@yahoo.com*

1071-3581/$34.00

Abbreviations	
CCR5	Chemokine receptor 5
SPECT	Single photon emission computed tomography
DAPTA	D-Ala-peptide T-amide
DOTA	1,4,7,10-tetraazacyclododecane-1,4,7,10-tetraacetic acid
HPLC	High performance liquid chromatography
$ApoE^{-/-}$	Apolipoprotein E knock-out
HFD	High fat diet
%ID·g	Percent injected dose per gram
p.i.	Post injection
ORO	Oil Red O

See related editorial, pp. 1179–1181

INTRODUCTION

Atherosclerosis leads to cerebrovascular and coronary artery disease, which continue to be major causes of mortality and morbidity.[1] Atherosclerosis is a chronic inflammatory process, beginning with endothelial dysfunction leading to abnormal subendothelial accumulation of oxidized lipids ('fatty streaks') and subsequent infiltration of inflammatory cells.[2,3] The influx of leukocytes is regulated by chemokines and their receptors.[2,3] Chemokine receptors CCR1, CCR2, CCR5, CXCR3, CXCR4, and CX3CR1 play a role in vascular inflammation and their expression varies during different stages of atherosclerotic plaque development.[2–4]

Early detection and follow-up of atherosclerosis is important in identification of patients for secondary prevention and later evaluation of therapy. ^{18}F-fluorodeoxyglucose (^{18}F-FDG) has been widely used to evaluate atherosclerosis in the aorta and the carotid and coronary circulations.[5,6] However, ^{18}F-FDG is a non-specific tracer with background uptake in skeletal muscle and myocardium which imposes technical challenges in lesion detection within the coronary arteries due to the small size of the vessels.[6,7] Diagnostic imaging agents targeting chemokine receptors may have greater specificity for detection of inflammation in atherosclerosis and identification of plaque stage.

CCR5 was initially known for its role as a co-receptor for human immunodeficiency virus infection of macrophages. However, new evidence supports the involvement of CCR5 in the development of atherosclerosis.[8] During the progression of atherosclerotic lesions, CCR5 is selectively upregulated in certain subsets of monocytes and facilitates their entry into the plaques,[2,8,9] which may provide an imaging target to identify the progress.[10,11] DAPTA, a threonine rich octapeptide (D-Ala-Ser-Thr-Thr-Thr-Asn-Tyr-Thr-NH_2), is a specific CCR5 antagonist (Figure 1).[12–14] Recently, a ^{64}Cu labeled DAPTA peptide and its nanoparticle derivative have been developed as PET imaging agents targeting CCR5.[11] These PET tracers were developed for evaluation of inflammation in a vascular injury model, with greater inflammation than usually observed in the apolipoprotein E double knock-out ($ApoE^{-/-}$) atherosclerosis mouse model.

We developed an ^{111}In labeled DAPTA peptide, targeting CCR5 as a SPECT imaging agent. SPECT imaging is more widely available than PET for cardiovascular imaging due to lesser cost. SPECT imaging can be performed with multiple emission energy windows .[15] Thus, dual isotope imaging is possible with SPECT using ^{111}In and ^{99m}Tc labeled tracers. For instance, the uptake of the myocardial perfusion tracer ^{99m}Tc-sestamibi can be used to co-register with the uptake of ^{111}In labeled white blood cells to localize infection in suspected endocarditis.[16] The new solid state cadmium-zinc-telluride SPECT systems have much greater count sensitivity and spatial and energy resolution[17] and are ideally suited for dual isotope molecular imaging. Here, we report the radiolabeling and characterization of ^{111}In labeled DAPTA, and in vitro cell uptake, *ex vivo* biodistribution, and autoradiography studies in an $ApoE^{-/-}$ atherosclerosis mouse model.

METHODS

$^{111}InCl_3$ was provided by Nordion Inc. (Ottawa, ON, Canada). The following experimental methods are provided as supplemental information: synthesis and characterization of DOTA-DAPTA, ^{111}In labeled DOTA-DAPTA and its cold indium analogue, serum stability of ^{111}In-DOTA-DAPTA, cell lines and cell culture conditions.

In vitro Cell Uptake Study in U87-CD4-CCR5 and U87-MG Cells

U87-MG and U87-CD4-CCR5 cells ($n = 5$ for both cell lines) were trypsinized and resuspended in binding buffer. One mL of the suspension containing 1×10^6 cells was incubated with 18.5 kBq of ^{111}In-DOTA-DAPTA at 37 °C for 1 hour or 2 hours. For the blocking experiment ($n = 5$), 10 μg (10 μL) of DAPTA was added before the tracer. After incubation, cells were centrifuged with 10% sucrose at 14,000 rpm for 5 minutes. The supernatant was collected in another vial and the cell pellets were washed with 10% sucrose and centrifuged again at 14,000 rpm for 5 minutes. The cell pellets, supernatant and washes were counted with a gamma well counter, and the percentage of binding calculated. The cell pellets were lysed with 0.5 mL lysis buffer at 4 °C for 20 minutes, and centrifuged at 14,000×g for 10 minutes. A Bradford assay was conducted to obtain the protein concentration. The cell

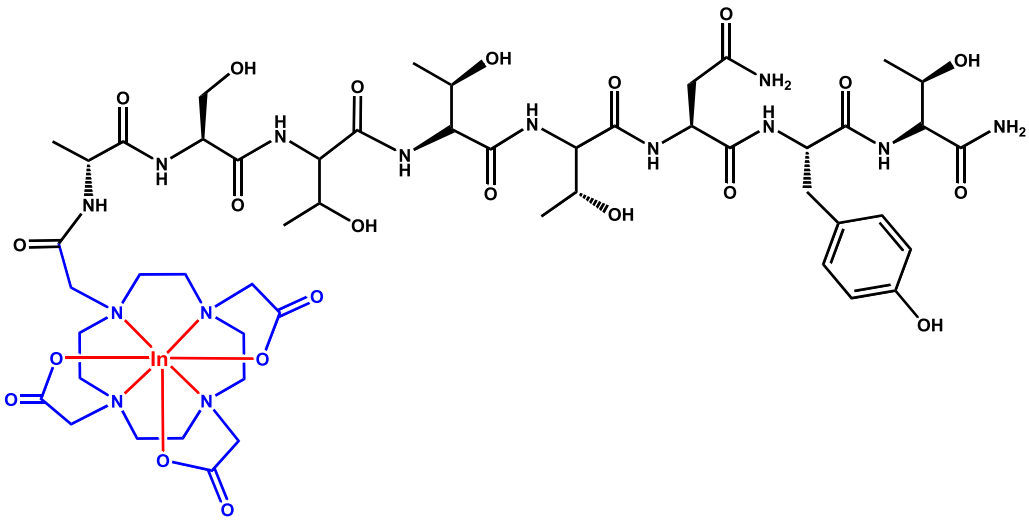

Figure 1. Structure of In-DOTA-DAPTA.

uptake was expressed as percentage of binding per mg of protein (%binding·mg).

Animals

All housing, handling and experimental procedures were conducted in compliance with the guidelines of the Canadian Council on Animal Care and with approval from the Animal Care Committee at the University of Ottawa.

Biodistribution Studies

Biodistribution studies were carried out on female C57BL/6 mice (Charles River Laboratories, MA, USA) weighing 18-22 g. The mice were anesthetized and maintained with isoflurane during the injection. ^{111}In-DOTA-DAPTA (4.8-7.4 MBq) was administered, and the mice were sacrificed at 30 minutes, 1 hour and 2 hours (n = 4 per time point) post injection (p.i.). The organs were extracted, weighed and analyzed for total gamma counts. The tissue uptake was decay corrected, and the percentage of injected dose per gram (%ID·g) was calculated.

Ex vivo En face Autoradiography, ORO Staining and Gamma Counting Studies with ApoE$^{-/-}$ Mice

Two month old female ApoE$^{-/-}$ mice were purchased from Charles River Laboratories and divided into three groups. The first group of mice were fed a chow diet for 7 months, while the second and third groups of mice were fed a western high fat diet (HFD) (TD.10885, Harlan Laboratories) for 2 months (n = 3 per group). Four month old C57BL/6 mice (n = 3), were used as normal controls. For the first and second groups of ApoE$^{-/-}$ mice and the C57BL/6 mice, ^{111}In-DOTA-DAPTA (37.0-55.5 MBq) was administered intravenously under anesthetic conditions. The third group of ApoE$^{-/-}$ mice (blocking group) received DAPTA peptide intravenously (0.3 mg in 0.15 mL saline) 1 hour before being injected with ^{111}In-DOTA-DAPTA. The mice were euthanized in a CO_2 chamber 1 hour p.i.. Using a Gilson Minipuls 2 peristaltic pump, the mice were perfused with 20 mL phosphate buffered saline followed by 10 mL of 10% formalin via left ventricular cannulation. Perfusate was drained from a cut within the right atrium. For *en face* experiments, the aorta was dissected from the heart at the base. The aortic tissues were flattened by a longitudinal cut ventrally through one side of the aortic wall and a second cut through the carotids and the innominate artery on the dorsal side until the aorta was split forming a Y-shaped structure.

The uptake and distribution of the tracer on aortic tissue was studied using digital autoradiography. *En face* specimens were immediately exposed to super resolution phosphor screens in an autoradiography cassette, as previously described.[18] After overnight exposure at room temperature, the screens were scanned with a Cyclone Phosphor Imager (Perkin Elmer). Images were analyzed using OptiQuant 5.0 software. For the measurement of radiotracer uptake by lesions in the ApoE$^{-/-}$ mice, regions of interest were drawn around the left side of the aortic arch on the Y-shaped *en face* samples where the lesions were seen. For the C57BL/6 mice with no lesions identified, the regions of interest were drawn around areas similar to the ApoE$^{-/-}$ mice. Equivalent sized areas (5-6 mm^2) were drawn for both ApoE$^{-/-}$ and C57BL/6 mice. The counts in Digital Light Units were measured, and converted to activity using a set of calibration standards with known activities, which were exposed and scanned on the same screen used for the aorta samples. The percentage injected dose (%ID) and activity density (%ID·m^2) were calculated and normalized by animal body weight to get %ID × kg·m^2, as previously described.[18]

The *en face* aortic tissue was photographed by an Infinity 2 digital camera mounted to a dissecting microscope. Lipid-

rich intraluminal lesions were stained with ORO and photographed again.[19] Each *en face* specimen was cut into two pieces, arch and descending aorta. The arch samples were weighed and counted on the gamma counter, and the percentage of injected dose per gram (%ID·g) calculated.

STATISTICAL METHODS

All data was presented as mean ± SD. To compare the cell uptake and biodistribution results between different groups, two-tailed unpaired Student *t*-tests were performed. One-way analysis of variance was used for analyzing the tracer uptake data from autoradiography and gamma counter studies for the four groups of mice, with post-hoc testing using Tukey's test. GraphPad PRISM (San Diego, CA) was used and differences at the 95% confidence level were considered significant.

RESULTS

Preparation of ^{111}In/^{115}In-DOTA-DAPTA and Serum Stability

DOTA-DAPTA was synthesized by reacting DOTA-NHS ester and DAPTA in 2:1 ratio, and purified by reverse phase High Performance Liquid Chromatography (HPLC). The conjugation efficiency was about 95%, as determined by HPLC. One DOTA chelate was conjugated to one DAPTA peptide as confirmed by High Resolution Mass Spectrometry (HRMS), and the proposed structure of DOTA-DAPTA is shown in Figure 1.

DOTA-DAPTA was radiolabeled with ^{111}In in pH 5.0 ammonium acetate buffer to achieve > 98% radiolabeling yield and radiochemical purity without purification. The specific activity was 70 MBq·nmol. After incubating the ^{111}In-DOTA-DAPTA with mouse serum at 37 °C for 2 hours, 90% of complex was intact as shown on HPLC, indicating its stability in vitro. The identity of the complex was confirmed by the same retention time on HPLC for the cold and ^{111}In labeled DOTA-DAPTA (Figure 2), and by High Resolution Mass Spectrometry (HRMS).

Cell Uptake Studies

In vitro cell uptake studies were conducted by incubating 18.5 kBq ^{111}In-DOTA-DAPTA with U87-CD4-CCR5 cells, which express high levels of CCR5. U87-MG cells were used as a negative control. The uptake of ^{111}In-DOTA-DAPTA in U87-CD4-CCR5 cells reached 0.88 ± 0.20 %binding·mg after 1 hour of incubation, and did not show significant change at 2 hours (0.90 ± 0.10 %binding·mg, P = NS) (Figure 3). The uptake in U87-MG cells was 0.21 ± 0.12 %binding·mg and 0.27 ± 0.12 %binding·mg at 1 hour and 2 hours incubations, respectively. These values were significantly lower than the uptake observed in U87-CD4-CCR5 cells ($P < .005$ at 1 hour and 2 hours). A blocking study was conducted at 2 hours time point by pre-incubating 10 μg of DAPTA before adding the tracer to the U87-CD4-CCR5 cells. The uptake of the blocking group (0.30 ± 0.04 %binding·mg) was three times lower than the non-blocked cells ($P < .005$).

Biodistribution Study

The biodistribution study in C57BL/6 mice (Figure 4) showed that ^{111}In-DOTA-DAPTA was cleared primarily through the renal system. The kidney uptake was high (4.27 ± 0.67 %ID·g) at 30 minutes and reduced to 2.48 ± 0.72 %ID·g at 2 hours p.i. ($P < .05$). Blood clearance was fast with initial uptake of 1.36 ± 0.29 %ID·g at 30 minutes p.i. and decreased dramatically to 0.14 ± 0.04 %ID·g at 2 hours p.i. ($P < .0002$). The tracer also cleared rapidly from other major organs, such as heart, lung, muscle, and femur. The spleen uptake was high, reaching 2.80 ± 1.34 %ID·g at 30 minutes p.i., slightly increased to 3.29 ± 1.34 %ID·g at 1 hour p.i. (P = NS), and slightly reduced to 2.14 ± 0.36 %ID·g at 2 hours p.i. (P = NS). The tracer also had significant accumulation in liver at 30 minutes (1.24 ± 0.57 %ID·g) and remained constant at 1 hour p.i. (1.15 ± 0.34 %ID·g, P = NS). The liver uptake reduced to 0.66 ± 0.21 %ID·g at 2 hours p.i. (P = NS).

Ex vivo Autoradiography Studies

The uptake of the tracer ^{111}In-DOTA-DAPTA in atherosclerotic lesions was evaluated in ApoE$^{-/-}$ mice using *ex vivo* autoradiography. The 9 month old ApoE$^{-/-}$ mouse with chow diet (Figure 5A) and the 4 month old ApoE$^{-/-}$ mouse with HFD (Figure 5B) developed several similar lesions in the aortic arch, as shown on the *en face* image, and the lesions had high lipid content shown by ORO staining. The autoradiographic images demonstrate the co-localization of ^{111}In-DOTA-DAPTA in the aortic lesions identified by *en face* and ORO imaging. For the 4 month old ApoE$^{-/-}$ HFD blocked mice (Figure 5C), several lesions were shown on the *en face* and ORO images. However, the autoradiography image showed much lower intensity of tracer uptake as compared to the non-blocked mouse. The 4 month old C57BL/6 mouse did not have any

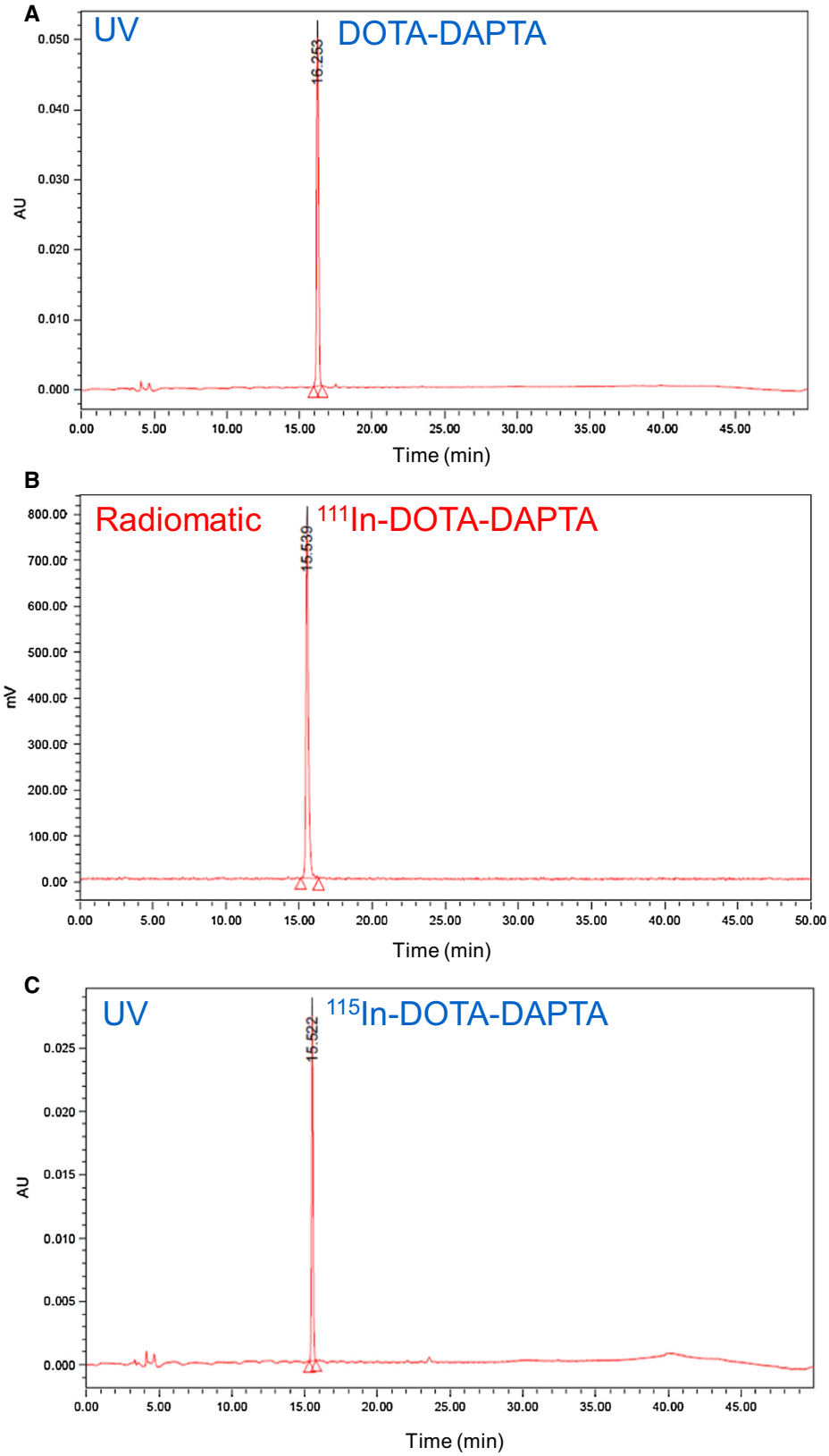

Figure 2. HPLC chromatograms. (**A**) DOTA-DAPTA (UV). (**B**) ^{111}In-DOTA-DAPTA (radiomatic). (**C**) ^{115}In-DOTA-DAPTA (UV) (UV: Ultraviolet).

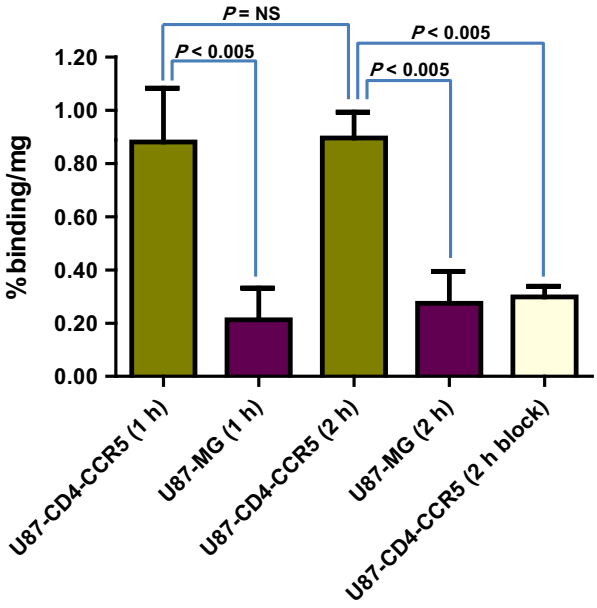

Figure 3. Cell uptake (%binding·mg) of ^{111}In-DOTA-DAPTA in U87-CD4-CCR5, U87-MG cells and U87-CD4-CCR5 cells incubated with DAPTA as the blocking agent ($n = 5$ each group).

aortic lesions on autoradiography, *en face* or ORO imaging (Figure 5D).

The lesion radiotracer uptake results measured with autoradiography (Figure 6A) and well counter (Figure 6B) were similar. The 9 month old ApoE$^{-/-}$ mice with chow diet and the 4 month old ApoE$^{-/-}$ mice with HFD had similar tracer uptake in the aortic lesions (P = NS). The uptake values for the 9 month old ApoE$^{-/-}$ mice with chow diet and the 4 month old ApoE$^{-/-}$ mice with HFD were significantly higher than the 4 month old C57BL/6 mice ($P < .0001$). The 4 month old ApoE$^{-/-}$ HFD mice pre-injected with blocking agent had approximately twofold lower tracer uptake compared to the same mice without blocking ($P < .001$). The blocked mice had higher tracer uptake than 4 month old C57BL/6 mice. The quantitative results in Figure 6 are consistent with the images in Figure 5.

DISCUSSION

We developed a diagnostic agent to target inflammation in atherosclerotic plaque using SPECT imaging. CCR5 was selected due to its important role in the

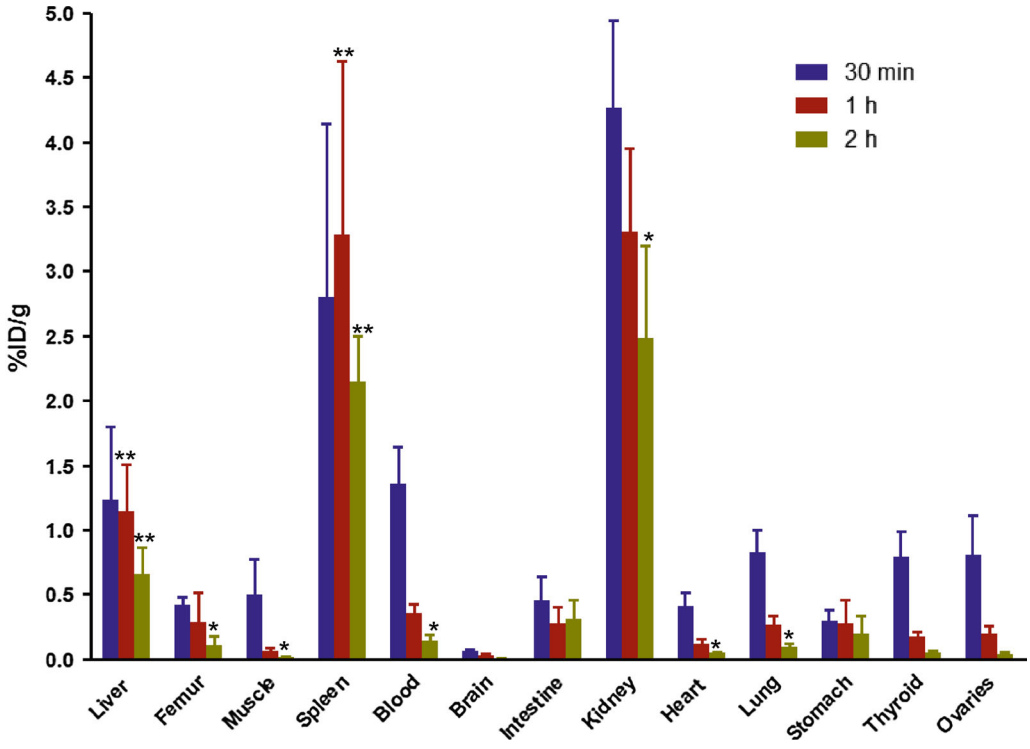

Figure 4. Biodistribution of ^{111}In-DOTA-DAPTA in C57BL/6 mice at 30 minutes, 1 h and 2 h p.i. * 30 min vs. 2 hr: femur: $P < 0.005$; muscle: $P < 0.02$; blood: $P < 0.0002$; kidney: $P < 0.05$; heart: $P < 0.002$; lung: $P < 0.0001$. ** For liver and spleen: 30 min vs. 1 hr and 30 min vs. 2hr: P = NS.

progression of atherosclerosis, especially during the late stage of the disease.[8,10] As an antagonist, DAPTA binds specifically to CCR5.[12,13] Moreover, various functional groups on the peptide can be easily modified and labeled with radioisotopes for SPECT or PET imaging.

In this study, the amine group on the alanine terminal of DAPTA was conveniently conjugated to DOTA, and DOTA-DAPTA was radiolabeled with ^{111}In with > 98% radiolabeling yield and radiochemical purity. We were able to achieve the specific activity of

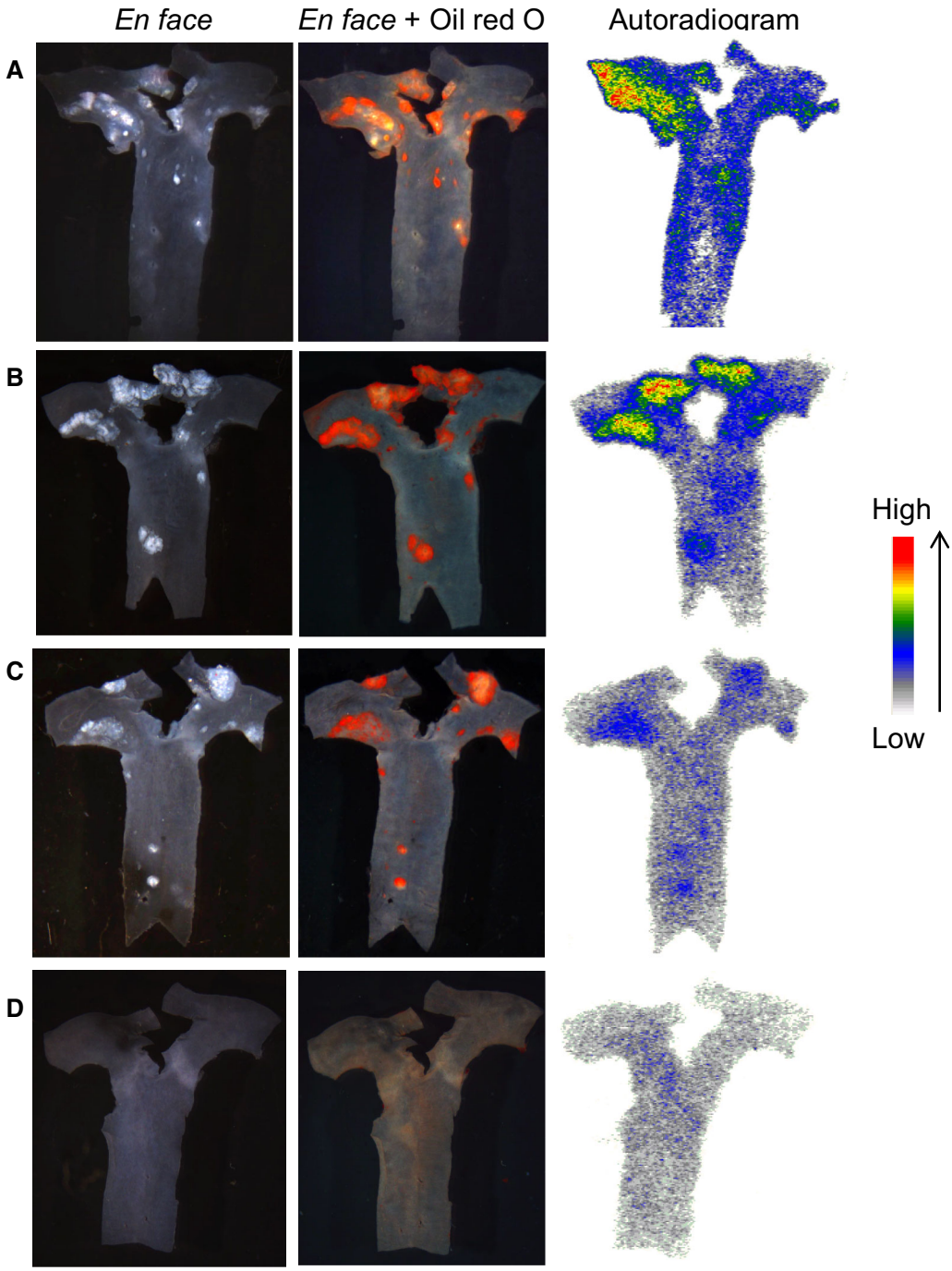

Figure 5. *En face*, ORO and autoradiographic images. (**A**) A 9 month old ApoE$^{-/-}$ mouse fed with chow diet. (**B**) A 4 month old ApoE$^{-/-}$ mouse fed with HFD for 2 months. (**C**) A 4 month old ApoE$^{-/-}$ mouse fed with HFD with the blocking agent DAPTA injected prior to tracer injection. (**D**) A 4 month old C57BL/6 mouse as the normal control.

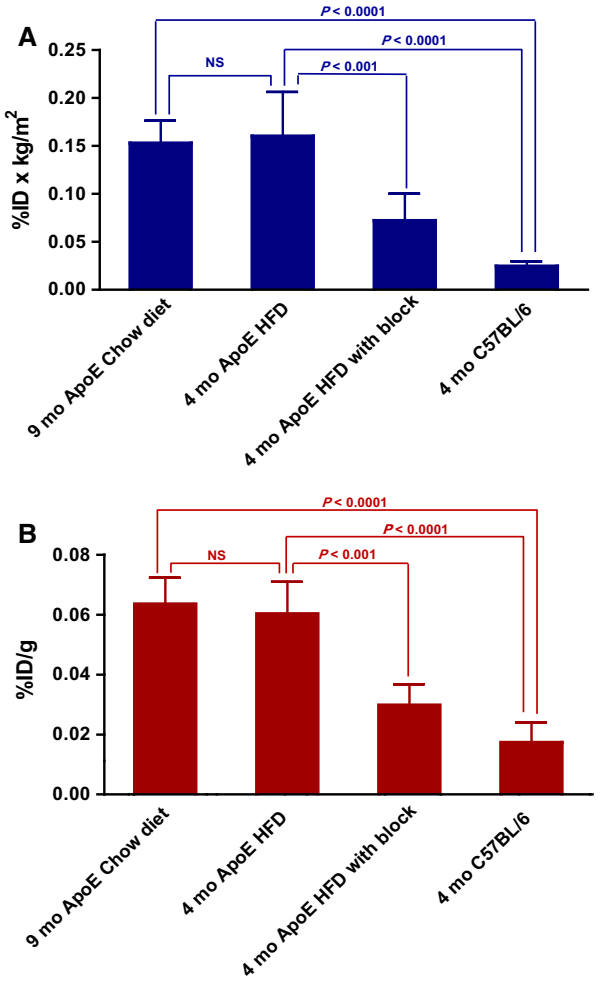

Figure 6. Comparison of lesion uptake of the four groups of mice (n = 3 each group). (1) 9 month old ApoE$^{-/-}$ mice fed with chow diet; (2) 4 month old ApoE$^{-/-}$ mice fed with HFD for 2 months; (3) 4 month old ApoE$^{-/-}$ mice with HFD pre-injected with DAPTA as the blocking agent; (4) 4 month old C57BL/6 mice as the normal control. (**A**) Autoradiography results. (**B**) Gamma counter results.

^{111}In-DOTA-DAPTA as high as 70 MBq·nmol, which is close to ^{64}Cu-DOTA-DAPTA (50.8 MBq·nmol) as previously reported.[11] Since no purification is needed, the tracer ^{111}In-DOTA-DAPTA can be prepared in a kit-formulation, which is beneficial for potential clinical application. The tracer is stable in vitro for 2 hours, determined by serum stability testing. $^{111}InCl_3$ is widely used as a bone marrow scintigraphy tracer.[20] The low bone uptake at 2 hours p.i. in the biodistribution study indicates low levels of free $^{111}InCl_3$, consistent with reasonable in vivo stability of the tracer (Figure 4).

The uptake of the tracer in U87-CC4-CCR5 cells was 4.2 and 3.3 times higher than the control U87-MG cells following 1 hour and 2 hours of incubation, respectively. More importantly, the uptake in U87-CD4-CCR5 cells was reduced by threefold when blocked by DAPTA peptide, suggesting that the uptake is receptor mediated (Figure 3).

The biodistribution study (Figure 4) demonstrated fast blood and renal clearance of ^{111}In-DOTA-DAPTA, which is typical for radiotracers constructed from peptides.[11,21,22] The tracer displayed high spleen and liver uptake, consistent with the reported ^{64}Cu-DOTA-DAPTA and ^{64}Cu-DOTA-DAPTA-comb,[11] and is related to the high concentration of chemokine receptors in the mononuclear phagocyte system. Another ^{64}Cu labeled compound ^{64}Cu-DOTA-vMIP-II, a tracer targeting multiple chemokine receptors, also had high liver and moderate spleen accumulation at 1 hour p.i..[22]

The tracer ^{111}In-DOTA-DAPTA was evaluated in an ApoE$^{-/-}$ atherosclerosis mouse model. The 9 month old ApoE$^{-/-}$ mice fed a chow diet and 4 month old ApoE$^{-/-}$ mice fed a HFD develop a significant amount of aortic lesions which have been well characterized.[23] *Ex vivo* autoradiographic imaging and gamma counter results showed that the two groups of mice had similar levels of ^{111}In-DOTA-DAPTA in their aortic lesions (Figure 6), and greater uptake compared to the 4 month old C57BL/6 mice. The 4 month old ApoE$^{-/-}$ HFD mice pre-injected with DAPTA peptide as a blocking agent showed 2-fold lower uptake of ^{111}In-DOTA-DAPTA compared to the same type of mice without the blocking agent. This suggests that the uptake of ^{111}In-DOTA-DAPTA is specific to chemokine receptor CCR5. The previous reported ^{64}Cu-DOTA-DAPTA-comb,[11] a radiotracer constructed from nanoparticle, was evaluated in a vascular wire-injury model in ApoE$^{-/-}$ mice. In the microPET imaging study, the ratio of ^{64}Cu-DOTA-DAPTA-comb uptake in the non-blocked vs blocked mice was approximately 2, similar to the ratio in our study. Interestingly, the ^{111}In-DOTA-DAPTA uptake in the blocked ApoE$^{-/-}$ HFD mice was higher than the same age C57BL/6 mice. Similarly, the ^{64}Cu-DOTA-DAPTA-comb uptake in the blocked mice was also higher than that in the C57BL/6 mice. This may be caused by the incomplete blockade due to the low dose of the blocking agent, which is limited by the maximum amount of blocking agents that can be administered to the mice.

At 1 hour p.i, the tracer uptake (%ID·g) in atherosclerotic aortas (Figure 6B) is lower than the blood uptake (Figure 4) due to differences in methodology. The biodistribution study (Figure 4) was performed with animal sacrifice, harvesting of organs and well counting, in comparison to atherosclerotic lesion uptake with animal sacrifice, harvesting, washing and weighing of aorta and post-autoradiography well counting (Figure 6B). The comparison between the blood and aorta uptake would not be valid. The standard

biodistribution ''cut and count'' procedure is challenging for small tissues like mice aortas without contamination from blood and surrounding tissues. In our study, the tracer uptake in atherosclerotic aortas was determined after autoradiography and acquisition of *en face* and Oil Red O stain images. The lower aortic uptake may be due to tissue washing to remove blood. The aortic weight may be increased due to the Oil Red O staining.

The tracer ^{111}In-DOTA-DAPTA shows quick pharmacokinetics, which is a common issue for peptide-based tracers, and may affect the sensitivity and contrast for in vivo imaging. Nanoparticles are well-known drug carriers that have been used widely to increase blood circulation time and enhance the efficiency of the therapeutic and imaging agents.[24] The previous study of ^{64}Cu-DOTA-DAPTA-comb demonstrated the imaging capability and superiority of the targeted nanoparticle tracer over the ^{64}Cu-DOTA-DAPTA peptide tracer for CCR5 receptor imaging.[11] Various types of nanoparticles can be adapted to incorporate the targeting moieties and radiotracers.[24] Our group has successfully developed nanoparticle platforms constructed from liposomes.[25] Our next step will be to conjugate ^{111}In-DOTA-DAPTA to liposomes and explore the advantages of the nanoparticle tracers.

A major limitation of the current study is the absence of in vivo SPECT imaging study in the ApoE$^{-/-}$ mice. The uptake of ^{111}In-DOTA-DAPTA was measured by *ex vivo* autoradiography imaging. Without nanoparticle conjugation, the tracer in its current form may not have enough target tracer uptake for SPECT imaging, due to the small size of the atherosclerotic lesions in the ApoE$^{-/-}$ mice. This challenge may be overcome by using atherosclerosis models in larger animals (rabbits, pigs and nonhuman primates).[26] An alternative model with greater target uptake and larger lesion size is the ApoE$^{-/-}$ mouse vascular injury model, which was used successfully in the previous study with ^{64}Cu-DOTA-DAPTA and its nanoparticle derivative.[11] Another limitation is the lack of histological data to demonstrate the inflammation and CCR5 expression in the aortic lesions, and their correlations with the tracer uptake.

NEW KNOWLEDGE GAINED

- The ApoE$^{-/-}$ mice had significant higher atherosclerotic lesion uptake of ^{111}In-DOTA-DAPTA, compared to the C57BL/6 mice.
- The blocking studies in both in vitro cell uptake in U87-CD4-CCR5 cells and *ex vivo* autoradiography imaging in ApoE$^{-/-}$ mice indicate that the uptake of ^{111}In-DOTA-DAPTA is specific to CCR5 receptor.

CONCLUSION

We have developed a novel tracer ^{111}In-DOTA-DAPTA that specifically targets CCR5. Future studies will warrant its potential as a SPECT agent for imaging inflammation in atherosclerosis.

Acknowledgements

This study was funded in part by the Ontario Research Fund (ORF RE07-021). Dr Wei Gan was supported through Mitacs Elevate Postdoctoral Fellowship. We are very grateful for the technical support from Animal Care technicians.

Authorship

Lihui Wei and Terrence Ruddy proposed the study objectives and designed the experiments. Lihui Wei, Wei Gan and Yin Duan performed the chemistry and radiochemistry synthesis and characterization experiments. Julia Petryk and Chantal Gaudet conducted the animal experiments. Lihui Wei and Maryam Kamkar performed the cell uptake studies. Lihui Wei and Terrence Ruddy analyzed the data and drafted the paper. All authors reviewed and provided comments for revising the paper.

Disclosure

Dr. Terrence Ruddy has received research grants from GE HealthCare and Advanced Accelerator Applications. Dr. Lihui Wei is a full-time employee of Nordion Inc. All other authors declare that they have no conflict of interest.

Research Involving Human Participants and/or Animals

The care and use of animals were conducted in compliance with the guidelines of the Canadian Council on Animal Care and with approval from the Animal Care Committee at the University of Ottawa. The procedures performed for this study did not involve human participants.

References

1. Weber C, Noels H. Atherosclerosis: Current pathogenesis and therapeutic options. Nat Med. 2011;17:1410-22.
2. Koenen RR, Weber C. Therapeutic targeting of chemokine interactions in atherosclerosis. Nat Rev Drug Discov. 2010;9:141-53.
3. Braunersreuther V, Mach F, Steffens S. The specific role of chemokines in atherosclerosis. Thromb Haemost. 2007;97:714-21.
4. Charo IF, Ransohoff RM. The many roles of chemokines and chemokine receptors in inflammation. N Engl J Med. 2006;354:610-21.
5. Rudd JH, Warburton EA, Fryer TD, Jones HA, Clark JC, Antoun N, et al. Imaging atherosclerotic plaque inflammation with [^{18}F]-fluorodeoxyglucose positron emission tomography. Circulation. 2002;105:2708-11.
6. Rudd JH, Hyafil F, Fayad ZA. Inflammation imaging in atherosclerosis. Arterioscler Thromb Vasc Biol. 2009;29:1009-16.

7. Quillard T, Libby P. Molecular imaging of atherosclerosis for improving diagnostic and therapeutic development. Circ Res. 2012;111:231-44.
8. Jones KL, Maguire JJ, Davenport AP. Chemokine receptor CCR5: From AIDS to atherosclerosis. Br J Pharmacol. 2011;162:1453-69.
9. Tacke F, Alvarez D, Kaplan TJ, Jakubzick C, Spanbroek R, Llodra J, et al. Monocyte subsets differentially employ CCR2, CCR5, and CX3CR1 to accumulate within atherosclerotic plaques. J Clin Invest. 2007;117:185-94.
10. Quinones MP, Martinez HG, Jimenez F, Estrada CA, Dudley M, Willmon O, et al. CC chemokine receptor 5 influences late-stage atherosclerosis. Atherosclerosis. 2007;195:e92-103.
11. Luehmann HP, Pressly ED, Detering L, Wang C, Pierce R, Woodard PK, et al. PET/CT imaging of chemokine receptor CCR5 in vascular injury model using targeted nanoparticles. J Nucl Med. 2014;55:629-34.
12. Ruff MR, Polianova M, Yang Q, Leoung GS, Ruscetti FW, Pert CB. Update on D-Ala-Peptide T-Amide (DAPTA): A viral entry inhibitor that blocks CCR5 chemokine receptors. Curr HIV Res. 2003;1:51-67.
13. Rosi S, Pert CB, Ruff MR, McGann-Gramling K, Wenk GL. Chemokine receptor 5 antagonist D-Ala-peptide T-amide reduces microglia and astrocyte activation within the hippocampus in a neuroinflammatory rat model of Alzheimer's disease. Neuroscience. 2005;134:671-6.
14. Polianova MT, Ruscetti FW, Pert CB, Ruff MR. Chemokine receptor-5 (CCR5) is a receptor for the HIV entry inhibitor peptide T (DAPTA). Antiviral Res. 2005;67:83-92.
15. Prior P, Timmins R, Petryk J, Strydhorst J, Duan Y, Wei L, et al. A modified TEW approach to scatter correction for In-111 and Tc-99m dual-isotope small-animal SPECT. Med Phys. 2016;43:5503-13.
16. Caobelli F, Wollenweber T, Bavendiek U, Kuhn C, Schutze C, Geworski L, et al. Simultaneous dual-isotope solid-state detector SPECT for improved tracking of white blood cells in suspected endocarditis. Eur Heart J. 2016;38:436-43.
17. Slomka PJ, Berman DS, Germano G. New cardiac cameras: Single-photon emission CT and PET. Semin Nucl Med. 2014;44:232-51.
18. Zhao Y, Kuge Y, Zhao S, Morita K, Inubushi M, Strauss HW, et al. Comparison of ^{99m}Tc-annexin A5 with ^{18}F-FDG for the detection of atherosclerosis in ApoE$^{-/-}$ mice. Eur J Nucl Med Mol Imaging. 2007;34:1747-55.
19. Kamkar M, Wei L, Gaudet C, Bugden M, Petryk J, Duan Y, et al. Evaluation of apoptosis with ^{99m}Tc-rhAnnexin V-128 and inflammation with ^{18}F-FDG in a low-dose irradiation model of atherosclerosis in apolipoprotein E-deficient mice. J Nucl Med. 2016;57:1784-91.
20. Agool A, Glaudemans AW, Boersma HH, Dierckx RA, Vellenga E, Slart RH. Radionuclide imaging of bone marrow disorders. Eur J Nucl Med Mol Imaging. 2011;38:166-78.
21. Liu Y, Abendschein D, Woodard GE, Rossin R, McCommis K, Zheng J, et al. Molecular imaging of atherosclerotic plaque with ^{64}Cu-labeled natriuretic peptide and PET. J Nucl Med. 2010;51:85-91.
22. Liu Y, Pierce R, Luehmann HP, Sharp TL, Welch MJ. PET imaging of chemokine receptors in vascular injury-accelerated atherosclerosis. J Nucl Med. 2013;54:1135-41.
23. Whitman SC. A practical approach to using mice in atherosclerosis research. Clin Biochem Rev. 2004;25:81-93.
24. Chen G, Roy I, Yang C, Prasad PN. Nanochemistry and nanomedicine for nanoparticle-based diagnostics and therapy. Chem Rev. 2016;116:2826-85.
25. Duan Y, Wei L, Petryk J, Ruddy TD. Formulation, characterization and tissue distribution of a novel pH-sensitive long-circulating liposome-based theranostic suitable for molecular imaging and drug delivery. Int J Nanomedicine. 2016;11:5697-708.
26. Getz GS, Reardon CA. Animal models of atherosclerosis. Arterioscler Thromb Vasc Biol. 2012;32:1104-15.